IEEE Access
Multidisciplinary ⋮ Rapid Review ⋮ Open Access Journal

Received 5 August 2024, accepted 14 August 2024, date of publication 19 August 2024, date of current version 29 August 2024.

Digital Object Identifier 10.1109/ACCESS.2024.3445528

RESEARCH ARTICLE

Roadside Intelligence: Efficient Channel Estimation for IRS-Aided mmWave Vehicular Communication

S. NANDAN, (Senior Member, IEEE), AND M. ABDUL RAHIMAN
LBS Institute of Technology for Women, APJ Abdul Kalam Technological University, Kerala 695016, India
Corresponding author: S. Nandan (nandans@ieee.org)

ABSTRACT Fifth-generation (5G) and beyond communication systems, assisted by Intelligent Reflecting Surfaces (IRS), often encounter hindrances such as unreliable connections, high energy usage, and prolonged latency. Channel estimation in IRS-aided systems is challenging in vehicular communication systems with roadside IRS units and fast-moving users. This paper proposes an efficient and low-complex channel estimation strategy for high-speed vehicular mmWave communication systems equipped with roadside IRS. The method consists of two stages, sensing and prediction, which aim to improve efficiency and accuracy under dynamic channel conditions. In the sensing phase, an initial assessment of channel characteristics is estimated by exploiting the sparse nature of the channel. We use the Compressive Sampling Matching Pursuit (CoSaMP) algorithm for accurate estimation with reduced computational complexity. The prediction stage consists of real-time tracking and prediction of the Angle of Arrival (AoA) and the Angle of Departure (AoD) using the Extended Kalman Filter (EKF). This ensures more accurate dynamic channel estimation based on predicted array response vectors without increasing the pilot overhead. Simulation results demonstrate that our proposed approach can offer precise channel estimation with significantly reduced training overhead.

INDEX TERMS Channel estimation, compressive sensing, high mobility, intelligent reflecting surface, millimeter wave communications, vehicular communication.

I. INTRODUCTION

Conventional wireless communication systems often function in an unpredictable environment where the line-of-sight (LOS) connection is unavailable primarily due to obstacles and the signals span on multiple paths, resulting in differences in time and angle before arriving at the destination. Hence, wireless systems may come across some issues, including low trustworthy communication, high energy consumption and increased latency. Recently, Intelligent Reflecting Surfaces (IRS) has evolved as an effective solution to subdue these hassles [1], [2], [3], [4]. IRS can carry out passive reflections to aid the wireless systems in satisfying the demands of the fifth generation (5G) and beyond communication systems. IRS stood out as an economical solution to achieve an intelligent and reconfigurable wireless transmission environment by adaptively adjusting signal reflections and subsequently enhancing the system performance. In specific, IRS is a controllable metasurface consisting of multiple passive reflective elements, and each of them will be able to independently modify the phase and/or the amplitude of the incident signal. Thus, the IRS can aid in circumventing obstacles and improving the multi-antenna/multiuser channel rank condition. Because of passive reflections, the IRS exhibits lower power consumption and hardware cost.

Most existing research on channel acquisition in IRS-aided wireless systems focused on static channel conditions, where the base station positions, IRS, and the user remain unchanging. In such static scenarios, acquiring the channel state information (CSI) through channel estimation algorithms is convincing. However, for the high mobility cases, the computational complexity and time requirement of such

The associate editor coordinating the review of this manuscript and approving it for publication was Mauro Fadda.

estimation methods are incredibly high, leading to the recurring communication outage for high-mobility users. Significant efforts are in the pipeline to achieve high-performance communications that involve high-speed vehicles. However, the increasing demands for the rapidly time-varying wireless channels due to high-mobility users are always the barrier in achieving the ultra-reliable, low-latency and high-capacity vehicle-to-everything (V2X) communications.

IRS-aided communication systems are well studied for various wireless systems with methodologies including multiple-input multiple-output (MIMO) [5], [6], orthogonal frequency division multiplexing (OFDM) [7], [8], [9], non-orthogonal multiple access (NOMA) [10], [11], and simultaneous wireless information and power transfer (SWIPT) [12]. Estimating accurate channel state information (CSI) in IRS-assisted systems is challenging due to the passive nature of IRS reflecting elements. There are two primary techniques for IRS channel estimation. The first approach is semi-passive IRS channel estimation, where fewer low-power active sensors are interlaced between passive reflective elements. The second approach is fully-passive IRS channel estimation, in which only passive reflective elements are engaged in the cascaded channel acquisition. In both methods, as the number of reflective elements increases, the training overhead increases, resulting in reduced throughput. Various techniques are available in the literature to address this, including element grouping in IRS [7], [13], anchor-aided channel acquisition [14], reference user-based methods [15], [16], and sparse channel estimation [17].

The knowledge of accurate channel state information (CSI) between BS-IRS-user is essential to achieve a high passive beamforming gain [18]. Since the IRS can perform passive reflections only, channel estimation in IRS systems is very challenging [19], [20], [21]. A possible practical strategy is to perform channel acquisition using pilot transmission [22]. Since the IRS has many passive reflective elements, high training overhead lowers the data transmission throughput. To tackle this issue, grouping adjacent reflecting elements with good spatial correlation into a subsurface is proposed in [8], [10]. Random beamforming is suggested in [23] to reduce the training overhead. Another method to reduce the training overhead using sparse matrix factorization is proposed in [24]. Information regarding the location and statistical CSI is also suggested [21].

Most existing works focus on time-invariant, slow-fading channels with low-mobility users. For high mobility cases, due to the random scattering of environment and vehicle velocity, the signal arrives after multiple reflections and the high Doppler frequency results in a fast-fading channel. This severely degrades the reliability of communication and the achievable rate. Transmitting pilot symbols during each time block for estimating the time-varying channel between the user and the IRS increases the training overhead. In addition, the continuous feedback of estimated channel coefficients from the base station to the IRS controller results in obsolete CSI as the channel varies rapidly due to the high mobility conditions. A method of placing IRSs at multiple fixed positions to aid high-speed communication is given in [25]. A channel estimation scheme for time-varying channels with Doppler shift is proposed in [26]. In [27], the authors proposed a roadside Intelligent Reflecting Surface (IRS)-aided vehicular communication system. By leveraging symmetrical IRS deployment and cooperation among nearby controllers, they introduced a two-stage channel estimation scheme for efficient passive beamforming. The design utilizes existing uplink pilots and achieves high IRS gain. The proposed method enhances communication throughput in high-speed vehicular scenarios. In [28], [29], and [30], the authors focused on two-timescale channel estimation and beamforming for IRS. These approaches aimed to reduce training and signaling overhead by leveraging the static base station (BS) to IRS channel. However, challenges remain: additional pilot symbols from users were required for IRS channel estimation, which leads to increased overhead and protocol modification requirements. Moreover, designing IRS reflection based on BS-acquired CSI introduced feedback delays which affects effectiveness in high-mobility scenarios. Authors in [31] and [32] propose a unified tensor-based approach that combines massive MIMO technology for efficient communication and sensing. They optimize the antenna system to handle both tasks simultaneously. By parameterizing the high-dimensional communication channel, they link channel state information with target parameters, including angular, delay, and Doppler dimensions. Additionally, they investigate tensor factorization's uniqueness conditions and determine the maximum number of resolvable targets. The authors in [33] proposed a tensor decomposition-based approach to estimate multi-path channel parameters, including azimuth and elevation angles, as well as complex gain coefficients in a general scenario without IRS. The proposed method enables the reconstruction of wireless channels between any pair of transmit and receive movable antenna positions. They introduced a two-stage Tx-Rx successive antenna movement pattern for pilot training and expressed received pilot signals as a third-order tensor. Factor matrices are obtained via canonical polyadic decomposition to estimate angle and gain parameters. However, for dynamic cascaded channels in the presence of IRS, the efficiency and computational complexity are still to be charted.

Efficient channel estimation methods are yet to be explored in time-varying channels with fast-moving users. In this paper, we propose a new, practically demanding, low-complex channel estimation strategy for improving the performance of high-speed vehicular communication mmWave systems with roadside IRS. The major contributions of this paper are outlined as follows.

The proposed strategy for estimating the cascaded channel in IRS-aided systems under dynamic channel conditions consists of two stages to improve the efficiency and accuracy of the assessment. The first stage is the sensing stage, which aims to establish an initial learning of the

channel characteristics. For this, we assume significantly fewer RF chains in the IRS controller side for various signal processing associated with the estimation, ensuring minimum power dissipation. We also consider that the channel between the base station and the IRS and between the IRS and the IRS controller is static. In the sensing stage, these static channels and the dynamic channel between the IRS and the fast-moving user are estimated. The CSI acquisition in this stage involves exploiting the sparse nature of the cascaded IRS mmWave channel. For this, Compressive Sampling Matching Pursuit (CoSaMP) algorithm [34] is employed for improved accuracy and reduced computational complexity. The second stage is the prediction stage, which involves real-time channel tracking and prediction of the Angle of Arrival (AoA) and Angle of Departure (AoD) is done using Extended Kalman Filter (EKF) [35], [36], thereby determining the array response vector at the IRS and the user. The dynamic channel estimation can be done based on the predicted array response vectors.

The rest of this paper is organized as follows. The system model and problem formulation are explained in Section II. In Section III, the proposed channel estimation methodology is explained in detail. The simulation results are given in Section IV and summarized in Section V.

II. SYSTEM MODEL AND PROBLEM FORMULATION

In this section, IRS-aided mmWave MIMO communication system with fast-moving users is presented. We then formulate the channel estimation as a compressive sensing-based sparse recovery problem with the aim to reduce the computational complexity and increase accuracy.

A. SYSTEM MODEL

Consider a narrow-band mmWave system with a uniform planar array type IRS furnished with N passive reflecting elements stationed to improve the system performance. The base station (BS) is set up with an N_t-antenna uniform linear array (ULA), and the user equipment (UE) is assumed to have a single antenna. We assume that the line-of-sight (LOS) path between the UE and the BS is blocked due to surrounding obstacles. We consider a high-mobility vehicular communication system supported by roadside IRSs deployed on both sides of the road. Without loss of generality, we assume one base station (BS) and a single mobile user with an intelligent reflecting surface (IRS) deployed on one side of the road, as shown in Figure 1. We assume the IRS-user channel with block-fading and is considered to stay roughly invariant during each block of transmission. However, due to the user's movement, the channel is supposed to change from block to block. Let each block duration be T_b, which is selected as small compared to the coherence time of the channel. To consider the influence of mobility, we consider K successive time blocks in one transmission frame. Between two consecutive

Blocks, the Angle of Arrival (AoA) and Angle of Departure (AoD) in the BS-IRS link are assumed to be constant,

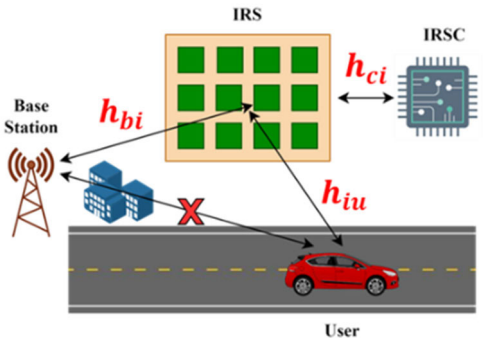

FIGURE 1. Roadside IRS-aided communication for serving high-speed vehicles.

while the same in the IRS-UE link varies due to the mobility of the user.

Let the complex baseband transmitted signal be $x_b(t)$ and the channel coefficient between the BS and the l^{th} reflecting element is denoted as $\alpha_l e^{-j\varphi_l}$, where $l \in \{1, 2, \ldots N\}$. The received signal $\tilde{\boldsymbol{y}}_l(t)$ at the l^{th} reflecting element is given by:

$$\tilde{\boldsymbol{y}}_{\boldsymbol{l}}(\boldsymbol{t}) = \mathrm{Re}\{\alpha_l e^{-j\varphi_l} \boldsymbol{x_b}(\boldsymbol{t})\, e^{j2\pi f_c t}\} \tag{1}$$

The reflection coefficient in the l^{th} reflecting element is given by β_l and let t_l be the time delay experienced by the incident signal, then the reflected signal from the l^{th} IRS element, $y_l(t)$ is given as:

$$\boldsymbol{y_l}(\boldsymbol{t}) = \beta_l \tilde{\boldsymbol{y}}_{\boldsymbol{l}}(\boldsymbol{t}-\boldsymbol{t_l}) \tag{2}$$

$$= \mathrm{Re}\{\beta_k \alpha_k e^{-j\varphi_k} \boldsymbol{x_b}(\boldsymbol{t}-\boldsymbol{t_k})\, e^{j2\pi f_c (t-t_k)}\} \tag{3}$$

Taking into consideration, the narrowband assumption, (3) can be rewritten as:

$$\boldsymbol{y_l}(\boldsymbol{t}) \approx \mathrm{Re}\{[\beta_l e^{-j\theta_l} \alpha_l e^{-j\varphi_l} \boldsymbol{x_b(t)}] e^{j2\pi f_c t}\} \tag{4}$$

where θ_l denotes the phase shift introduced by the l^{th} reflecting element. Thus,

$$\boldsymbol{y_l}(\boldsymbol{t}) \approx \mathrm{Re}\{\beta_l e^{-j\theta_l} \boldsymbol{x_b'}(\boldsymbol{t})\, e^{j2\pi f_c t}\} \tag{5}$$

where $x_b'(t) = \alpha_l e^{-j\varphi_l} x_b(t)$ is the baseband equivalent of $\tilde{\boldsymbol{y}}_l(t)$. Equation (5) can thus be re-written as:

$$\boldsymbol{y_l}(\boldsymbol{t}) \approx \mathrm{Re}\{\boldsymbol{x_b^o}(\boldsymbol{t})\, e^{j2\pi f_c t}\} \tag{6}$$

where $\boldsymbol{x_b^o}(\boldsymbol{t}) = \beta_l e^{-j\theta_l} \boldsymbol{x_b'}(\boldsymbol{t})$ is the baseband equivalent of $\boldsymbol{y_l}(\boldsymbol{t})$. Within a single transmission block, from the l^{th} reflecting element to the mobile UE, the IRS reflected signal will undergo similar narrowband flat fading and the baseband channel coefficient is given by $\alpha_l^r e^{-j\varphi_l^r}$. During the same transmission block, the received passband signal at the UE via the IRS, $\boldsymbol{y_l^r}(\boldsymbol{t})$ is thus given as:

$$\boldsymbol{y_l^r}(\boldsymbol{t}) = \mathrm{Re}\{[\alpha_l e^{-j\varphi_l} \beta_l e^{j\theta_l} \alpha_l^r e^{-j\varphi_l^r} \boldsymbol{x_b(t)}] e^{j2\pi f_c t} \tag{7}$$

The CSI in the cascaded channel model in (7) can be written as $\boldsymbol{H_{bi}^*} = \alpha_l e^{-j\varphi_l}$ and $\boldsymbol{H_{iu}^{[q]^*}} = \alpha_l^r e^{-j\varphi_l^r}$, where $\boldsymbol{H_{bi}^*}$ corresponds to the channel coefficients between BS and l^{th} reflecting element and $\boldsymbol{H_{iu}^{[q]^*}}$ denotes the corresponding

IRS-UE link in an arbitrary selected block q. Equation (7) can thus be re-written as

$$\boldsymbol{y}_l^r(\boldsymbol{t}) = \mathrm{Re}\{[\boldsymbol{H}_{\boldsymbol{bi}}^* \beta_l e^{j\theta_l} g_l \boldsymbol{x_b}(t)] e^{j2\pi f_c t}\} \tag{8}$$

$$= \mathrm{Re}\{\boldsymbol{y_l}(\boldsymbol{t})\, e^{j2\pi f_c t}\} \tag{9}$$

Neglecting coupling effects, the resultant baseband signal from all the N reflecting elements can thus be shown as:

$$\boldsymbol{y}(\boldsymbol{t}) = \left(\sum_{l=1}^{N} \boldsymbol{H}_{\boldsymbol{bi}}^* \beta_l e^{j\theta_l} \boldsymbol{H}_{\boldsymbol{iu}}^{[q]^*}\right) \boldsymbol{x_b}(t) \tag{10}$$

$$= \boldsymbol{H}_{\boldsymbol{bi}}^{\boldsymbol{H}} \boldsymbol{Q} \boldsymbol{H}_{\boldsymbol{iu}}^{[q]} \boldsymbol{x_b}(t) \tag{11}$$

where channel coefficients $\boldsymbol{H}_{\boldsymbol{bi}}^{\boldsymbol{H}} = [\boldsymbol{H}_{\boldsymbol{bi1}}^*, \boldsymbol{H}_{\boldsymbol{bi2}}^* \ldots, \boldsymbol{H}_{\boldsymbol{biN}}^*]$, $\boldsymbol{H}_{\boldsymbol{iu}}^{[q]} = \left[\boldsymbol{H}_{\boldsymbol{iu1}}^{[q]}, \boldsymbol{H}_{\boldsymbol{iu2}}^{[q]} \ldots, \boldsymbol{H}_{\boldsymbol{iuN}}^{[q]}\right]^T$ and the reflection matrix $\mathrm{Q} = diag(\beta_1 e^{j\theta_1}, \beta_2 e^{j\theta_2} \ldots, \beta_N e^{j\theta_N})$, is a complex diagonal matrix of size $N \times N$. The diagonality is because of the assumption that there is no coupling effect among IRS elements and the elementwise reflections are purely independent. The above model can be now be extended to the Multiple Input Multiple Output (MIMO) case with N_t transmit antennas, N IRS elements and a single receive antenna and the received signal can now be expressed as:

$$\boldsymbol{Y} = \left(\boldsymbol{H}_{\boldsymbol{BI}}^{\boldsymbol{H}} \boldsymbol{Q} \boldsymbol{H}_{\boldsymbol{IU}}^{[q]}\right) \boldsymbol{X} + \boldsymbol{N} \tag{12}$$

where, $H_{BI} \in \mathbb{C}^{N_t \times N}$ and $H_{IU} \in \mathbb{C}^{N \times 1}$. The incident signal shall get scattered if the dimensions of object are comparable to the wavelength, but here the dimensions of reflecting elements are much larger than the wavelength of signal and because of the same, the incident signal shall get reflected. In general, the channel through IRS can thus be expressed as:

$$\boldsymbol{H}_{\boldsymbol{IRS}} = \sum_{l=1}^{L} \alpha_l^{IRS} \boldsymbol{a}_{\boldsymbol{R}}^{[q]}\left(\vartheta_l^r, \varphi_l^r\right) \boldsymbol{a}_{\boldsymbol{T}}^*\left(\vartheta_l^t, \varphi_l^t\right) \tag{13}$$

where α_l^{IRS} denotes the path gain corresponding to the l^{th} IRS-aided path. a_T and a_R represent the array response vector at the transmitter and the receiver respectively with azimuth angle ϑ and elevation angle φ. An IRS can govern the angles of arrival ϑ_l^r and φ_l^r. For convenience, we will split the entire channel into two different parts, the first one being the BS-IRS channel and the latter one being the IRS-UE channel. The array response vector at the IRS is obtained as the Kronecker product of steering vector functions along two perpendicular directions of the IRS plane. The IRS – user channel during the q^{th} block is assumed to be a time varying channel due to the high mobility of the user as well as the relatively shorter distance with respect to the serving IRS. The overall cascaded channel in the q^{th} block, i.e., $\boldsymbol{H}_{\boldsymbol{BI}}^{\boldsymbol{H}} \boldsymbol{Q} \boldsymbol{H}_{\boldsymbol{IU}}^{[q]}$ may thus be represented as $\boldsymbol{H}^{[q]}$. We also assume that there is no direct link between the user and the base station.

B. PROBLEM FORMULATION

In this section, we will formulate the channel estimation problem for an IRS-aided mmWave system. By intelligently altering the phase shifts of each reflecting element, the signal received at the IRS will be directed to the user equipment without involving any time delay. Our primary task is to estimate the cascaded channel $\boldsymbol{H}$. It is important to note that for a mmWave channel, the number of multipath components, L is often less than the dimension of the channel matrix. This results in a sparse matrix with very few non-zero coefficients. Precise estimation of channels is difficult in IRS-assisted cascaded mmWave systems. The channel state information (CSI) can be estimated using pilot symbol transmission in a conventional wireless communication system. However, the reflecting elements in IRS systems are passive; hence, they do not possess any signal-processing capability. This makes channel estimation challenging in practice. Most existing research works consider perfect CSI for designing the precoding and phase shift matrices at the base station (BS) and IRS, respectively. However, this presumption is hard to achieve in practice. Many estimation techniques and algorithms were proposed to handle these concerns.

Considering the sparse character of mmWave, where the L number of multipath is typically much less than the channel dimensions, the channel matrix between the base station and the IRS can be expressed in more detail as:

$$\boldsymbol{H}_{\boldsymbol{BI}} = \left(\boldsymbol{U}_{\boldsymbol{x}} \otimes \boldsymbol{U}_{\boldsymbol{y}}\right) \boldsymbol{A}_{\boldsymbol{L}} \boldsymbol{U}_{\boldsymbol{BS}}^{\boldsymbol{H}} \tag{14}$$

where $\otimes$ denotes the Kronecker product and $\boldsymbol{U}_{\boldsymbol{x}}$, $\boldsymbol{U}_{\boldsymbol{y}}$ are defined with its columns having the one-dimensional steering vector functions a_x and a_y respectively. The IRS is assumed as an $N_x \times N_y$ uniform planar array (UPA). The steering vector functions depend on the antenna/element spacing, angles of arrival/departure and the signal wavelength. $\boldsymbol{A}_{\boldsymbol{L}}$ is a diagonal matrix with L non-zero values which denotes the channel path gains. $\boldsymbol{H}_{\boldsymbol{BI}}$ can be rewritten as

$$\boldsymbol{H}_{\boldsymbol{BI}} \triangleq \boldsymbol{U}_{\boldsymbol{IRS},b} \boldsymbol{A}_{\boldsymbol{L}} \boldsymbol{U}_{\boldsymbol{BS}}^{\boldsymbol{H}} \tag{15}$$

Similarly, the BS – IRS channel can be represented as:

$$\boldsymbol{H}_{\boldsymbol{IU}}^{\boldsymbol{H}} \triangleq \boldsymbol{U}_{\boldsymbol{user}} \boldsymbol{A}_{\boldsymbol{L}'} \boldsymbol{U}_{\boldsymbol{IRS},u}^{\boldsymbol{H}} \tag{16}$$

where, $\boldsymbol{U}_{\boldsymbol{user}}$, $\boldsymbol{U}_{\boldsymbol{IRS},u}$ and $\boldsymbol{A}_{\boldsymbol{L}'}$ are also defined as in the above case. $\boldsymbol{U}_{\boldsymbol{user}}$ and $\boldsymbol{U}_{\boldsymbol{IRS},u}$ depends on array response vectors $a_{IRS,u}$ and a_{user}, which in turn depends on the Angle of Arrival (AoA) and Angle of Departure (AoD) between the user-IRS link. The cascaded channel can now be expressed as:

$$\boldsymbol{h} = vec(\boldsymbol{H}) = vec\left(\boldsymbol{U}_{\boldsymbol{IRS},b} \boldsymbol{A}_{\boldsymbol{L}} \boldsymbol{U}_{\boldsymbol{BS}}^{\boldsymbol{H}} \boldsymbol{Q} \boldsymbol{U}_{\boldsymbol{user}} \boldsymbol{A}_{\boldsymbol{L}'} \boldsymbol{U}_{\boldsymbol{IRS},u}^{\boldsymbol{H}}\right) \tag{17}$$

$$\begin{aligned}
\boldsymbol{h} &\triangleq \left(\boldsymbol{U}_{\boldsymbol{IRS},u}^{\boldsymbol{T}} \otimes \boldsymbol{U}_{\boldsymbol{IRS},b}\right) vec\left(\boldsymbol{A}_{\boldsymbol{L}} \boldsymbol{U}_{\boldsymbol{BS}}^{\boldsymbol{H}} \boldsymbol{Q} \boldsymbol{U}_{\boldsymbol{user}} \boldsymbol{A}_{\boldsymbol{L}'}\right) \\
&\triangleq \left(\boldsymbol{U}_{\boldsymbol{IRS},u}^{\boldsymbol{T}} \otimes \boldsymbol{U}_{\boldsymbol{IRS}}\right) \left(\boldsymbol{A}_{\boldsymbol{L}'}^{\boldsymbol{T}} \otimes \boldsymbol{A}_{\boldsymbol{L}}\right) vec\left(\boldsymbol{U}_{\boldsymbol{BS}}^{\boldsymbol{H}} \boldsymbol{Q} \boldsymbol{U}_{\boldsymbol{user}}\right) \\
&\triangleq \left(\boldsymbol{U}_{\boldsymbol{IRS},u}^{\boldsymbol{T}} \otimes \boldsymbol{U}_{\boldsymbol{IRS}}\right) \left(\boldsymbol{A}_{\boldsymbol{L}'}^{\boldsymbol{T}} \otimes \boldsymbol{A}_{\boldsymbol{L}}\right) \left(\boldsymbol{U}_{\boldsymbol{user}}^{\boldsymbol{T}} \otimes \boldsymbol{U}_{\boldsymbol{BS}}^{\boldsymbol{H}}\right) vec(\boldsymbol{Q}) \\
&\triangleq \left(\boldsymbol{U}_{\boldsymbol{IRS},u}^{\boldsymbol{T}} \otimes \boldsymbol{U}_{\boldsymbol{IRS}}\right) \left(\boldsymbol{A}_{\boldsymbol{L}'}^{\boldsymbol{T}} \otimes \boldsymbol{A}_{\boldsymbol{L}}\right) \boldsymbol{U} \boldsymbol{q}
\end{aligned} \tag{18}$$

where, $\boldsymbol{U} = \left(\boldsymbol{U}_{\boldsymbol{user}}^{\boldsymbol{T}} \otimes \boldsymbol{U}_{\boldsymbol{BS}}^{\boldsymbol{H}}\right)$ and $\boldsymbol{q} = vec(\boldsymbol{Q})$. Based on this the received signal can be written as:

$$\begin{aligned}
\boldsymbol{y} &= vec(\boldsymbol{Y}) = vec(\boldsymbol{H})\boldsymbol{X} + vec(\boldsymbol{N}) \\
&\triangleq \left(\boldsymbol{U}_{\boldsymbol{IRS},u}^{\boldsymbol{T}} \otimes \boldsymbol{U}_{\boldsymbol{IRS}}\right) \left(\boldsymbol{A}_{\boldsymbol{L}'}^{\boldsymbol{T}} \otimes \boldsymbol{A}_{\boldsymbol{L}}\right) \boldsymbol{U} q \boldsymbol{X} + n
\end{aligned} \tag{19}$$

where, $n = vec(N)$. If we consider the precoder matrix P, then:

$$\begin{aligned} y &= P\left(U_{IRS,u}^{T} \otimes U_{IRS}\right)\left(A_{L'}^{T} \otimes A_{L}\right) U q X + n \\ &\triangleq (U^{T} \otimes q^{T} \otimes (X^{T} \otimes P))\left(U_{IRS,u}^{T} \otimes U_{IRS}\right) \\ &\quad \times \left(A_{L'}^{T} \otimes A_{L}\right) U + n \\ &\triangleq (U^{T} \otimes q^{T} \otimes (X^{T} \otimes P))\left(U_{IRS,u}^{T} \otimes U_{IRS}\right) h' + n \\ &\triangleq \Psi h' + n \end{aligned} \tag{20}$$

where, $\Psi = (U^{T} \otimes q^{T} \otimes (X^{T} \otimes P))\left(U_{IRS,u}^{T} \otimes U_{IRS}\right)$ and $h' = A_{L'}^{T} \otimes A_{L}$. Because of very few non-zero entries, h' is sparse in nature and the channel estimation thus tends to be a sparse recovery problem based on compressive sensing. The traditional estimation methods are meant for time-invariant slow fading channels. In this research, we consider a highly mobile user, which is moving at a velocity v. This results in a Doppler shift in the frequency and, thereby, a significant decrease in the coherence time (T_c). As coherence time goes much below the symbol duration, the channel quickly fades and becomes time-varying. This condition is applicable for IRS-aided vehicular communication systems with high-mobility users.

As shown in Figure 1, H_{BI} and H_{CI} are assumed to be static channels, and H_{IU} is considered time-varying because of user mobility. If we go for a pilot-based channel estimation, the training overhead increases especially for time varying channels as we need to transmit pilots before the start of each block of transmission and this eventually results in the reduction in throughput. To the best of our knowledge, fully efficient and tangible methods are not available in the literature to estimate highly mobile time-varying IRS-aided 5G mmWave channels. Even though some sparse estimation methods are available in the literature, performance–complexity trade-off exists for all techniques due to rapid changes in the channel and the estimation is extremely challenging.

III. PROPOSED CHANNEL ESTIMATION SCHEME

In this paper, we propose a 2-stage channel estimation strategy developed to improve the performance of mmWave wireless communication systems. The first estimation stage involves pilot-based estimation of channels H_{CI}, H_{BI} and H_{IU} using computationally efficient method with Compressive Sampling Matching Pursuit (CoSaMP) algorithm. In the second stage, real-time tracking and prediction of Angle of Arrival (AoA) and Angle of Departure (AoD) is done using Extended Kalman Filter (EKF) and are used to predict the array response vectors subsequently. The proposed methodology aims to optimize channel estimation by integrating computationally efficient sparse estimation methods and accurate predictive modelling.

The first stage of the proposed channel estimation methodology involves three steps. The dedicated channel between the IRS and the corresponding IRS controller (IRSC) is estimated in the first step. The IRS controller (IRSC) transmits pilot symbols to the IRS with 180° reflection, which helps to assess the channel vector H_{CI}. Subsequently, in the second step, the IRSC transmits pilots to the Base Station (BS) via the IRS. The BS then computes the IRSC-IRS-BS static cascaded channel $H_{CI} - H_{BI}$ based on the received signal and provides feedback to the IRSC through a backhaul link. Since H_{CI} is known at the IRSC, H_{BI} can be computed at the IRSC based on this feedback information via the backhaul link. The third step utilizes an efficient sparse estimation technique, Compressive Sampling Matching Pursuit (CoSaMP), to estimate the initial channel hiu between the fast-moving user and the IRS. Pilot-based estimation is done in the initial time block, and the information is then used for subsequent predictions.

In the second stage, the algorithm focuses on real-time tracking and channel characteristic prediction, which is critical for dynamic environments. The system initially predicts azimuth angle ϑ_{k+1} and elevation angle φ_{k+1} at both the IRS and the user, commencing with an initial value of $k = 1$ and then incrementing iteratively. The Extended Kalman Filter (EKF) is utilized for this iterative prediction process. The array response vectors are subsequently computed based on the predicted values, thereby calculating the channel matrix $H_{IU}(k+1)$ between the fast-moving user and the IRS at the BS. These computed channel coefficients are then fed back to the IRSC. The next step involves updating the prediction variables after K-blocks of transmission by communicating pilot symbols from the user to the IRS. This ensures continued adaptation and improvement of the prediction model. The iterative process continues effectively and integrates the two stages to obtain a computationally efficient and accurate channel estimation strategy.

To estimate the Doppler shift in the proposed IRS-aided mmWave system simulation, key system parameters such as the carrier frequency, vehicle velocity, and angle of motion relative to the line of sight (LOS) are initially defined. The Doppler shift (f_d) is calculated using the formula: $(v \times f_c \times \cos\theta)/c$. The baseband signal is generated using QPSK modulation and known pilot symbols are inserted at regular intervals. The communication channel is modeled to include the Doppler effect. At the receiver end, the pilot symbols are extracted from the received signal and used correlation method to estimate the frequency offset. This involved comparing the received pilot symbols with the known transmitted ones to determine the frequency shift, thereby estimating the Doppler shift. This process allows us to accurately assess the impact of the Doppler effect on the performance of mmWave communication system.

A. SPARSE CHANNEL ESTIMATION USING CoSaMP

In this sub-section, we will discuss the estimation of sparse channels using the Compressive Sampling Matching Pursuit (CoSaMP) algorithm. CoSaMP is a sparse recovery method that integrates the benefits of both greedy algorithms and convex programs. It is beneficial for sparse

channel estimation with multiple paths. Conventional estimation approaches consider closely distributed channel impulse responses. This may lead to elongated training sequences, resulting in inefficient throughput and bandwidth. If the channel impulse response is sparse, compressed sensing can be used to trim the length of training sequences. Cascaded IRS mmWave channel impulse response has very few prevalent taps and considerable near-zero or zero taps. CoSaMP incorporates both greedy algorithm and convex program approaches. Even though greedy algorithms are easy to execute, they lack stability. On the other hand, convex programs are stable but complex for practical implementation. CoSaMP forms a balance between these two methods.

From the received samples, CoSaMP iteratively estimates the sparse channel. It initializes the estimates by assigning all channel coefficients to zero. It then identifies the support set using a greedy method. The support set indicates the indices of non-zero channel coefficients. A convex optimization problem is then solved to fine-tune the estimates within the determined support set. After solving the convex optimization problem, the estimates are updated by merging the results obtained from the greedy method and the convex optimization step. This is continued until convergence. One of the major advantages of CoSaMP is its simplicity, inherited from greedy algorithms which results in reduced computational complexity. The algorithm also exhibits stability in practical scenarios. CoSaMP is suitable for practical implementations, especially in scenarios where computational resources are limited. If the training matrix $\boldsymbol{X}$ satisfies the condition:

$$(1-\epsilon_S)\,\|\boldsymbol{h}\|_2^2 \leq \|\boldsymbol{Xh}\|_2^2 \leq (1+\epsilon_S)\,\|\boldsymbol{h}\|_2^2 \qquad (21)$$

for the channel matrix $\boldsymbol{h}$, then the training matrix is said to satisfy the Restricted Isometry Property (RIP) of order $\boldsymbol{S}$. In addition to this if the $\boldsymbol{2S}$-sparse channel matrix $\boldsymbol{h}$ satisfies $\epsilon_s \leq \sqrt{2}-1$, then the CoSaMP algorithm can be used to design a channel estimator that satisfies the condition

$$\left\|\boldsymbol{h}-\hat{\boldsymbol{h}}\right\|_2 \leq \boldsymbol{Cmax}\left\{\delta, 1\Big/\sqrt{S}\left\|\boldsymbol{h}-\hat{\boldsymbol{h}}_{\boldsymbol{2S}}\right\|_1 + \|\boldsymbol{n}\|_2\right\} \qquad (22)$$

Here $\hat{\boldsymbol{h}}_{\boldsymbol{2S}}$ is the $\boldsymbol{2S}$-sparse approximation of channel matrix $\boldsymbol{h}$.

The CoSaMP algorithm in the proposed methodology picks whole dominant taps in each iteration and diminishes the assessment error after each iteration. The channel estimation algorithm using CoSaMP is as shown in Algorithm 1. The Compressive Sampling Matching Pursuit (CoSaMP) algorithm starts with an initialization phase in which the estimate $\boldsymbol{h}^{(0)}$ is set to zero. The received signal $\boldsymbol{y}$ is set as the initial residual $\boldsymbol{r}^{(0)}$. It then identifies the $\boldsymbol{2S}$ dominant information from the last residual $\boldsymbol{r}^{(t-1)}$. A sparse support set, $\boldsymbol{\Omega_t}$ is formed, which consists of the indices of $\boldsymbol{2S}$ components. The algorithm then moves on to solve a least squares problem. It tries to find the best fit for the signal support. The estimator then focuses only on the most relevant information. It keeps only the $\boldsymbol{2S}$ most essential pieces of the signal estimate

Algorithm 1 CoSaMP

Input: Observation vector y, Measurement matrix $\boldsymbol{\Phi}$, noise vector n
Initialization: Set the current estimate $\boldsymbol{h}^{(0)}$ to zero. Initialize the residual $r^{(0)} = \boldsymbol{y}$ and set the iteration counter $t = 1$.
Repeat:

1. Sparse Support set Estimation:
   i. Identify the $2S$ largest components (in magnitude) of the current residual $r^{(t-1)}$.
   ii. Form a support set $\boldsymbol{\Omega_t}$ containing the indices of these $2S$ components.
2. Least Squares Approximation:
   i. Solve the least squares problem to obtain an estimate of the signal support: $\hat{\boldsymbol{h}}_{\Omega_t} = \arg min_x \left\|\boldsymbol{y} - \boldsymbol{\Phi}_{\boldsymbol{\Omega_t}}\boldsymbol{h}\right\|_2^2$. Here, $\boldsymbol{\Phi}_{\boldsymbol{\Omega_t}}$ is the submatrix of $\boldsymbol{\Phi}$ formed by the columns corresponding to $\boldsymbol{\Omega_t}$.
3. Thresholding:
   i. Keep only the S largest components (in magnitude) of $\hat{\boldsymbol{h}}_{\boldsymbol{\Omega_t}}$ and set the rest to zero. This enforces sparsity in the estimated signal.
4. Support Union:
   i. Form the updated support set $\boldsymbol{\Omega_t}$ by combining the non-zero indices from the current estimate with the support indices obtained from the least squares step.
5. Update the Estimate:
   i. Solve the least squares problem using the updated support set to obtain the new estimate $\boldsymbol{x}^{(t)}$:
   ii. $\hat{\boldsymbol{h}}_{\boldsymbol{\Omega_t}}^{(t)} = \arg min_x \left\|\boldsymbol{y} - \boldsymbol{\Phi}_{\boldsymbol{\Omega_t}}\boldsymbol{h}\right\|_2^2$
   iii. Set the components outside of the support set Ω_t to zero.
6. Update Residual:
   i. Update the residual: $\boldsymbol{r}^{(t)} = \boldsymbol{y} - \boldsymbol{\Phi h}^{(t)}$.
7. Check Convergence:
   i. Check for convergence conditions. This could involve checking the change in the estimate or the residual.

Output: The final output is the estimate $\boldsymbol{h}^{(t)}$.

$\hat{\boldsymbol{h}}_{\boldsymbol{\Omega_t}}$ and discards the less relevant rest. In the support union step, the algorithm updates and expands its list of crucial indications $\boldsymbol{\Omega_t}$, by integrating new results. It then refines the estimate by solving another least square problem, which gives an improved signal estimate $\boldsymbol{h}^{(t)}$. The next step involves updating the residual and checking for convergence. CoSaMP is thus a reliable algorithm with simplicity, accuracy, and efficiency.

The algorithm gathers this notion repetitively to match the target. A residual is induced after each iteration. Samples are updated as the algorithm proceeds, and this is reflected in the present residual components. This step delivers an indicative consent for the next approximation. We employ the samples to assess the support set using the least squares. This process is repeated iteratively until convergence. The algorithm delivers an $\boldsymbol{S}$-sparse evaluation whose ℓ_2 error matches the scaled ℓ_1 error of the $(\boldsymbol{S}/2)$-sparse approximation to the channel coefficients. Yet, uncertainty may emerge in the presence of noise. However, the error bound is fundamentally optimal. Without noise, the algorithm is capable of retrieving an s-sparse channel with increased accuracy, but the performance adulterates as noise increases.

TABLE 1. Comparative analysis of various compressive sensing algorithms.

Algorithm	Complexity	Remarks
Orthogonal Matching Pursuit (OMP) [37]	$\mathcal{O}(s \cdot n \cdot m)$	Simple but sensitive to noise
Matching Pursuit (MP) [38]	$\mathcal{O}(n^2 \cdot m)$	Slow convergence
Stagewise Orthogonal Matching Pursuit (StOMP) [39]	$\mathcal{O}(s \cdot n \cdot m)$	Good for high dimensional data
Regularized Orthogonal Matching Pursuit (ROMP) [40]	$\mathcal{O}(s \cdot n \cdot m)$	Can handle noisy signals
Expander Matching Pursuits (EMP) [41]	$\mathcal{O}\left(s \cdot \log\frac{n}{s}\right)$	Not suitable for large dimensional data
Sparse Matching Pursuits (SMP) [42]	$\mathcal{O}\left(s \cdot \log\frac{n}{s}\log r\right)$	Accuracy not guaranteed always
Belief Propagation [43]	$\mathcal{O}(n \cdot log^2 n)$	Global optimality
Basis Pursuit (BP) [44]	$\mathcal{O}(n^3)$	Accuracy is good
Least Absolute Shrinkage and Selection Operator (LASSO) [45]	$\mathcal{O}(n^3)$	May get biased solution
Improved OMP (Double structured Orthogonal Matching Pursuit (DS-OMP) [46]	$\mathcal{O}(n \cdot m)$	Reduced complexity and better accuracy than OMP
Compressive Sampling Matching Pursuit (CoSaMP) [35]	$\mathcal{O}(n \cdot m)$	Very good accuracy even with noise

The *Reconstruction Signal to Noise Ratio* ($R-SNR$) is given by

$$\boldsymbol{R-SNR = 10log_{10}\frac{\|h\|_2}{\left\|h-\hat{h}\right\|_2}} \tag{23}$$

Interestingly, the number of iterations is almost fixed if we need a high reconstruction SNR. This occurs even if the estimate has a very broad dynamic range. The Compressive Sampling Matching Pursuit (CoSaMP) algorithm is selected for the proposed work based on the comparative analysis of various compressive sensing algorithms and is given in Table 1. After carefully considering the same, it is observed that Compressive Sampling Matching Pursuit (CoSaMP) has reduced computational complexity compared to other methods in the case of IRS-aided communication systems.

B. REALTIME PREDICTION OF AoA AND AoD USING EXTENDED KALMAN FILTER

In this sub-section, we will discuss the real-time tracking & prediction of AoA (φ) & AoD (ϑ) in the IRS-user link using Extended Kalman Filter (EKF). In an Intelligent Reflecting Surface (IRS)-assisted mmWave system with a fast-moving user, it is very crucial to track and predict the angle of arrival (AoA) and angle of departure (AoD) at the IRS or the user or both in real-time. The channel between the user and the IRS is dynamic due to the user's movement. Real-time tracking and prediction enable accurate time-varying channel estimation, which is essential for selecting parameters such as beamforming vectors, precoding matrices and optimal power allocation. Most of the current research on beam positioning in IRS-aided systems concentrated on the static context. In such stationary cases, it is likely to attain the channel state information (CSI) via various existing channel estimation algorithms. When the user starts moving at a very high velocity, the complexity and estimation time of such algorithms increases. This eventually leads to communication outage. The traditional filter-based algorithms are to track and predict the AoA and the AoD based on their initial estimation. However, in the RIS-aided communication system, it is difficult to acquire the AoD and AoA at the IRS due to the absence of active RF chains.

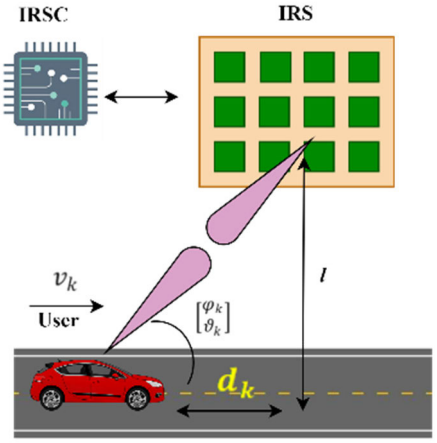

FIGURE 2. Physical model of IRS-aided communication with high-speed vehicles.

A two-timescale estimation is possible without obtaining the real angle knowledge at the IRS. A more practical approach in static channels is the estimation of the cascaded angles at the IRS instead of azimuth and elevation angles. By estimating cascaded angles, the system can infer the overall directionality of the signal propagation, which is crucial for optimizing signal reflection and transmission at the IRS. However, this approach is challenging, especially in dynamic scenarios. Our proposed work uses the Extended Kalman

Filter (EKF) algorithm for tracking and predicting the arrived and (or) departed beams. The state model is hinged on the AoA and AoD. The system for beam tracking and prediction in vehicular communication scenarios using EKF is modelled based on the state evaluation model and observation expression. In the existing approach, the state model is assumed to be linear, which is not the case in a vehicular communication environment. We also consider factors such as the initial position and speed of the vehicle as well as the span of transmission blocks. The proposed algorithm introduces EKF for tracking and predicting angles in

Algorithm 2 Extended Kalman Filter

State Vector: State Vector: $a_k = \begin{bmatrix} \varphi_k \\ \vartheta_k \end{bmatrix}$ where a_k is the state vector at time k, which includes the parameters we are estimating (φ- AoA, & ϑ - AoD).
Dynamic Model (State Transition): $a_k = f\left(a_{k-1} + v_{k-1}\right) + w_{k-1}$, where f is the state transition function to predict how the state will evolve from time *k-1* to k, w_{k-1} is the process noise, v_{k-1} is the control input or system input at time $k-1$ (velocity of the user).
Measurement Model: it relates the state to the measurements received from the system. $z_k = m\left(a_k\right) + u_k$, where m is the measurement function and u_k is the measurement noise.
Initialization: Set state estimate $\hat{a}_0$ and the error covariance matrix P_0.
Repeat:

1. State Transition:
   i. State prediction: $\hat{a}_0^- = f\left(a_{k-1} + v_{k-1}\right) + w_{k-1}$.
   ii. Error Covariance Prediction: $\boldsymbol{P_k^-} = \boldsymbol{F_k P_{k-1} F_k^T} + \boldsymbol{Q_{k-1}}$. Here $\boldsymbol{F_k} = \frac{\partial f}{\partial a}$ at (a_{k-1}, v_{k-1}) is the Jacobian matrix of f w.r.t a and $\boldsymbol{Q_{k-1}}$ is the process noise covariance matrix.
2. Measurement model: $\boldsymbol{z_k} = m\left(a_k\right) + u_k$
   i. Measurement Residual: $\boldsymbol{y_k} = \boldsymbol{z_k} - m(\hat{a}_k^-)$.
   ii. Measurement Jacobian: $\boldsymbol{M_k} = \frac{\partial m}{\partial a}$ at $\hat{a}_k$
   iii. Kalman Gain: $\boldsymbol{K_k} = \boldsymbol{P_k^- M_k^T}\left(\boldsymbol{M_k P_k^- M_k^T} + \boldsymbol{R_k}\right)^{-1}$, where $\boldsymbol{R_k}$ is the measurement noise covariance matrix.
   iv State Update: $\hat{a}_k = \hat{a}_k^- + K_k y_k$
   v Error Covariance Update: $\boldsymbol{P_k} = \left(\boldsymbol{I} - \boldsymbol{K_k M_k}\right)\boldsymbol{P_k^-}$
3. Iterative Process:
   i. Repeat steps 1 and 2 for each new measurement as the user's AoA & AoD change with time.

Output: The final output is the estimate $\hat{a}_k$.

a vehicle-to-infrastructure (V2I) scenario. We also consider position and velocity as the state variables and the algorithm exhibits reduced computational complexity. The tracking and prediction algorithm using EKF is as shown in Algorithm 2.

In the initialization step, an introductory state vector estimate and an error covariance matrix are fixed. Following this, it predicts the evolution of the state through an iterative process. The dynamic model integrates both a state transition function and process noise. Fine-tuning of the estimates is done using the measurements received from the system. The measurement model relates the state to the measurements. A critical step here is the linearization of the nonlinear functions using Jacobian matrices. The extent to which the prediction and measurement influence the updated state estimate is determined by the Kalman Gain. It is calculated based on the prediction error and uncertainty in the measurement.

This iterative method persists with each new measurement and refines the state estimate and error covariance. The extended Kalman filter handles the uncertainties in both system dynamics and measurements. Overall, it is versatile and practical in handling non-linear systems. The vehicular communication system using mmWave technology in the presence of IRS exhibits moderate non-linearity in the state evolution model. We assumed additive Gaussian noise mainly because of the absence of a direct path between the BS and the moving user. The system also showcases the kinematic characteristics of vehicular communications. These issues can be particularized by investigating the evolution of angles of the moving user.

TABLE 2. Comparative analysis of various tracking algorithms.

Algorithm	Advantages	Limitations
Kalman Filter [47]	Optimal estimation by minimizing MSE, low computational complexity, applied in a recursive manner	Limited to linear systems, Gaussian noise assumption & sensitive to inaccuracies in the system model
Unscented Kalman Filter [48]	Handles non-linearities and does not require computation of Jacobian matrices as in EKF.	Can be computationally more expensive than EKF, especially for high-dimensional state spaces. Sensitivity is same as EKF and also assumes Gaussian noise.
Particle Filter [49]	Suitable for non-linear and non-Gaussian systems. Adaptable to a wide range of system models & does not assume linearity in the system	Computationally expensive, reduced estimation accuracy.
Extended Kalman Filter [36]	Applicable to moderately non-linear systems and has moderate computational complexity. Maintains the recursive update characteristic of KF.	Sensitive to the choice of initial conditions and may converge to local minima. Assumes Gaussian noise attributes & moderate computational complexity.

We considered a uniform linear array (ULA) at both destinies of the communication. The dissimilarity between the array response vectors and beamforming angles at both sides of the communication constitutes the tracking error. We keep this error to a minimum so that we can track the beam for a longer time. A comparative analysis of various tracking algorithms is shown in Table 2. Since the IRS-aided mmWave channel is modelled as non-linear, Extended Kalman Filter-based prediction shall outperform since the same is appropriate for moderately non-linear systems, and it assumes Gaussian noise attributes and also maintains moderate computational complexity. The limitation of EKF based prediction is its inability to handle systems with non-Gaussian noise characteristics.

The proposed method has several advantages. Firstly, it remarkably lowers pilot overhead. It also streamlines operations and offers an efficient methodology. This reduction in pilot overhead is essential for improving the overall performance of the system. Moreover, the use of the Extended Kalman Filter (EKF) brings a notable increase in efficiency. The EKF can effectively address non-linear systems. This flexibility guarantees improved performance, especially in dynamic environments. The use of the EKF brings a significant increase in efficiency by effectively addressing the non-linear dynamics. This guarantees improved performance and ensures reliable communication in time varying channels.

In the context of research involving time-varying channels with fast-moving vehicles, the Extended Kalman Filter (EKF) outperforms the standard Kalman Filter (KF). Specifically, when dealing with non-linear channel models in the presence of an Intelligent Reflecting Surface (IRS), the EKF excels. It achieves this by linearizing around an estimate of the current mean and covariance. While the KF is optimal for linear systems with Gaussian noise, the EKF provides more accurate estimates for non-linear systems. Consequently, for the given application, the EKF strikes a balance between accuracy and reduced complexity compared to alternatives like the Unscented Kalman Filter or Particle Filter.

Integrating the proposed sparse channel estimation strategy of IRS based systems in existing 5G infrastructure needs careful planning and coordination. Since accurate channel models are crucial, it is important to consider both line-of-sight (LOS) and non-line-of-sight (NLOS) paths and model the channel between the base station (BS), IRS, and static/dynamic user equipment (UE). Proper installation of IRSs at strategic locations (e.g., walls, ceilings) within the coverage area and ensure proper alignment and orientation for optimal reflection are to be done. Along with this, implementation of control algorithms to adjust IRS phase shifts dynamically and coordinate IRS actions with BS and UE for coherent beamforming is crucial. Pilot signals shall be used initially as proposed in the algorithm for channel estimation. In addition to normal communication, allocate resources (frequency, time, power) for IRS reflection and optimize the resource allocation jointly with BS and UE. IRSs are to be connected to the network via wired or wireless backhaul. Proper steps are to be done to avoid interference between IRSs and neighboring cells. Collaboration with standardization bodies (e.g., 3GPP) is needed to define IRS-related protocols for practical deployment.

IV. SIMULATION RESULTS

In this section, we discuss the performance of the proposed channel estimation technique for IRS-assisted MIMO systems in time-varying channels. We consider ULA at both BS and fast-moving UE sides and operating over the mmWave frequency band. The proposed scheme's performance is experimentally compared with several existing channel estimation algorithms that rely on pilot-based estimation. To assess the effectiveness of the cascaded channel estimation schemes, we considered the Normalized Mean Square Error (NMSE) and the achievable spectral efficiency (SE). The NMSE will assess the accuracy of channel estimation. The below expression represents it:

$$NMSE \triangleq \frac{\left\|\boldsymbol{h}-\hat{\boldsymbol{h}}\right\|_2^2}{\|\boldsymbol{h}\|_2^2} \tag{24}$$

where $\hat{\boldsymbol{h}}$ is the estimate and $\boldsymbol{h}$ is the actual channel. It is evident that if the value of NMSE is less, the estimated channel $\hat{\boldsymbol{h}}$ is closer to the actual channel $\boldsymbol{h}$. Assumptions made for executing the simulation are listed in Table 3.

TABLE 3. Simulation parameters.

Parameters	Values
No. of transmit antennas	32
No. of receive antennas (N_r)	2
No. of IRS elements (N)	64
No. of RF chains	8
No. of pilot symbols (L_p)	32
No. of iterations	100
No. of channel taps (L)	4
Doppler shift (f_D)	1 kHz - 10 kHz
Fading type	Rayleigh
Block length (L_B)	300 μs
Coherence time	100 μs - 3 ms
Channel estimation category	Cascaded (Fully-passive)
Modulation scheme	QPSK
Error Correction schemes	Nil
MSE calculation	$\frac{1}{N_t N_r}\left\|\widehat{\boldsymbol{H}}-\boldsymbol{H}\right\|^2$
Simulation software	Python 3.8

The simulation results of Normalized Mean Square Error (NMSE) versus Signal to Noise Ratio (SNR) for various algorithms for the estimation and tracking of time varying IRS channel with number of transmitting antennas at the BS $N_t = 32$, number of receiving antennas at the user equipment $N_r = 2$ and number of IRS elements $N = 64$, is shown in figure 3. It is observed that for time varying channel, the accuracy of the proposed two stage method reduces significantly at all SNR ranges. Considerable decrease is observed especially at low-SNR regions, thereby assuring the reliability of the communication system even at worse channel conditions.

The improvement in the system performance may be due to the fact that the conventional schemes adopt suboptimal paths and may easily get stuck in suboptimal solutions. CoSaMP performs well in accurately estimating sparse IRS channels with reduced computational complexity. This method will be beneficial, especially when the number of reflecting elements is very large. By exploiting the channel sparsity, CoSaMP efficiently estimates the channel state information even in the presence of noise and interference. Furthermore, the use of the Extended Kalman Filter (EKF) for channel tracking and prediction ensures improved accuracy even though the system is non-linear. The baseline schemes considered here are Orthogonal Matching Pursuit (OMP) and Improved OMP. Unlike OMP, which selects only one atom (basis function) per iteration, the proposed method selects multiple atoms simultaneously and this improves channel estimation accuracy, especially when the channel is sparse and high dimensional. The proposed scheme efficiently handles noise and interference due to its robustness. In the case of time varying channels with fast moving users, OMP and Improved OMP may struggle with noise and non-ideal conditions.

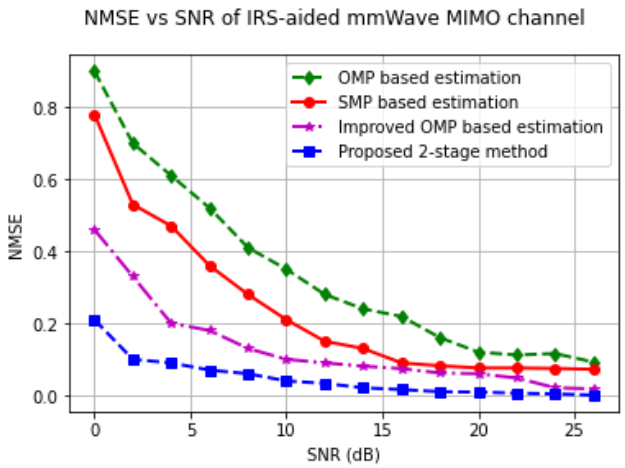

FIGURE 3. Simulation results of NMSE vs SNR (in dB) with $N_t = 32$, $N_r = 2$ and $N = 64$.

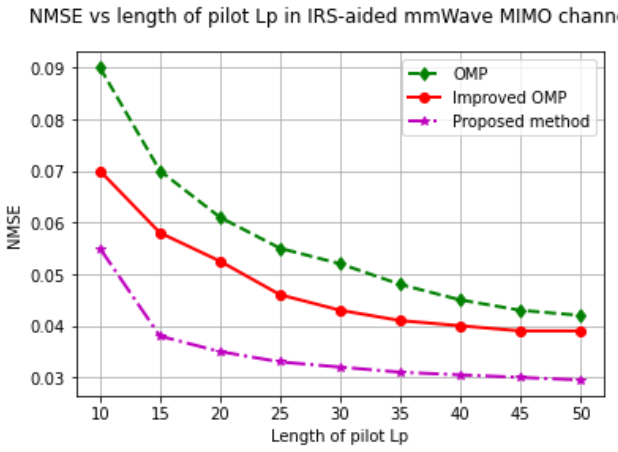

FIGURE 4. Simulation results of NMSE vs pilot sequence length L_p.

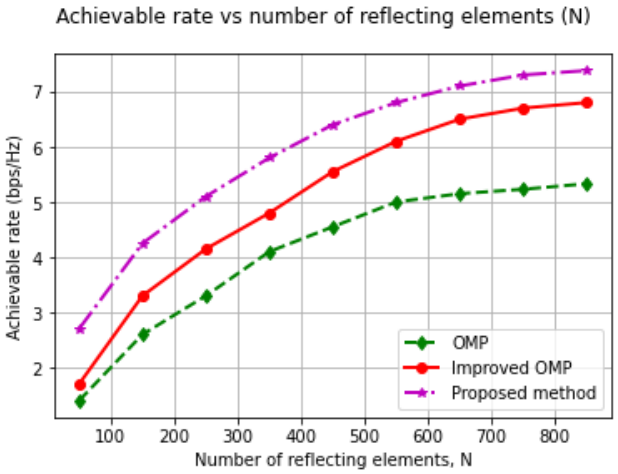

FIGURE 5. Simulation results of achievable rate vs pilot sequence length L_p.

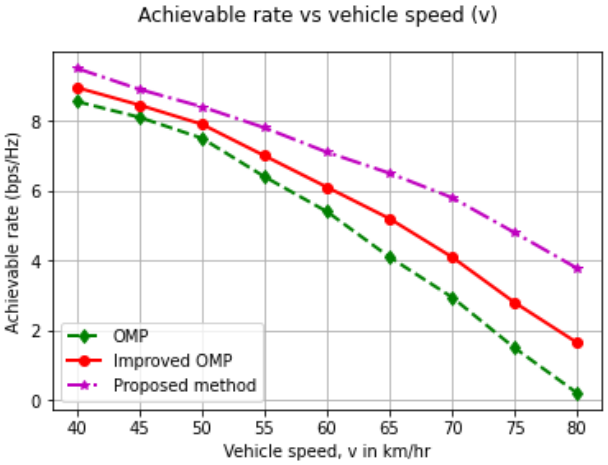

FIGURE 6. Simulation results of achievable rate vs velocity of the user equipment, v.

Next, we analyze the effect of the pilot sequence length L_p on the effectiveness of the algorithms. Figure 4 shows the performance of the system for various pilot sequence lengths at SNR = 40dB. It is evident that the proposed method achieves better performance compared to conventional schemes. This means that the proposed method requires minimal training length, and that too during the initial transmission block only. Prediction by EKF will be done during the subsequent blocks.

This significantly reduces the overhead complexity and improves the data rate of the system. We also observed that the improvement in NMSE is negligible for L_p values greater than around 35. The proposed method's synergy between CoSaMP and EKF, along with minimal training requirements, places it as a better choice for sparse IRS channel estimation compared to traditional OMP-based approaches. We also analyzed the relationship between the achievable rate and the number of reflecting elements N, with transmit power $P_t = 15$ dBm. We have observed that the attainable rate increases as the number of reflecting elements increases. For the proposed method, the achievable rate is much higher for a dynamic environment than for conventional methods.

The EKF-based predictor accurately predicts the φ & ϑ, which results in the system's improved efficiency. This happens without compromising the pilot overhead requirement, and the beamforming gain increases as the number of reflecting elements increases. We also analyzed the achievable rate versus the speed of the user equipment with the number of reflecting elements fixed at $N = 250$ for the same transmit power $P_t = 20$ dBm. For a fixed pilot overhead, due to the decreasing value of coherence time, as velocity increases, the time duration left for the transmission of data reduces. This results in a significant reduction in the achievable rate at higher velocities as shown in figure 6. Compared to the existing conventional schemes, the proposed method achieves a higher data rate due to its ability to overcome pilot overhead problem.

It is interesting to note that the achievable rate reduces drastically for the conventional techniques like OMP, if the user equipment is moving at a very high velocity of approximately 80km/hr for a given transmit power of $P_t = 20$ dBm. It is also worth noting that as velocity increases, the rate

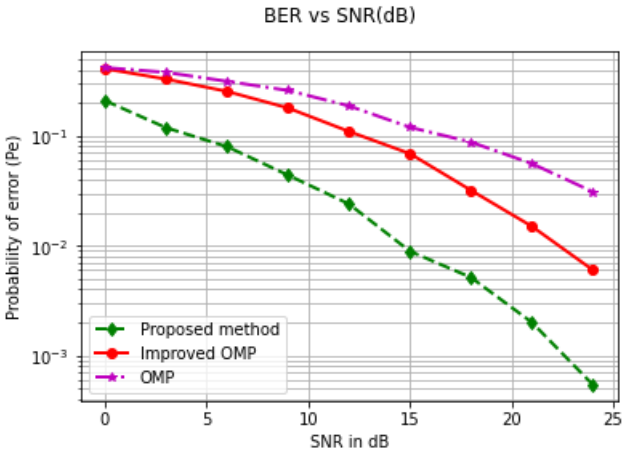

FIGURE 7. BER vs SNR curve of IRS channel with user travelling at a speed of 40km/hr.

at which the achievable rate declines also increases. This is due to the reduction in coherence time at higher Doppler frequencies. The bit error rate obtained for an IRS aided system with a fast-moving user with velocity $v = 40$ km/hr for different values of signal to noise ratio (SNR) in dB scale is shown in figure 7. It is evident from the obtained figure that the proposed system gives significant improvement in the system reliability compared to conventional techniques. Additionally, the increased system performance is attained with a reduced computational complexity which is achieved due to the reduced pilot overhead of the proposed system.

It is observed from figure 7 that, for a given probability of error of 0.4×10^{-2}, the proposed system attains almost 7dB SNR improvement. This clearly indicates the efficiency of the proposed system compared to the conventional methods. Additionally, it is worth to note that the complexity of the proposed system is approximately $O(N_t \cdot N_r)$, which is much less compared to traditional OMP with pilot-based transmission. In the latter scheme, $O(K \cdot P \cdot N_t \cdot N_r)$, where K is the number of blocks per symbol duration and P is the number of pilot symbols. The proposed method can also be used for the estimation of separate channels with much reduced computational complexity since separate channels possess lower dimensions than cascaded ones.

V. CONCLUSION

In this paper, we studied a roadside IRS-assisted dynamic vehicular communication system. An efficient, two-stage channel estimation technique was proposed, making fast-moving vehicular communication more efficient, which in turn leads to improved communication throughput and reliability. Our proposed two-stage method ascertained its remarkably enhanced performance over conventional methods under a more general environment. Simulation results indicated that the NMSE performance of the proposed methodology outshines the existing conventional OMP-based algorithms. Additionally, the pilot overhead of the proposed method is much less than that of the existing methods. The proposed method excels in accuracy and computational efficiency, making it ideal for applications where real-time response is less critical. This allows for high-quality results without sacrificing processing speed. More refined or improved algorithms for IRS channel estimation and prediction are worthy of further research.

REFERENCES

[1] M. Di Renzo, A. Zappone, M. Debbah, M.-S. Alouini, C. Yuen, J. de Rosny, and S. Tretyakov, "Smart radio environments empowered by reconfigurable intelligent surfaces: How it works, state of research, and the road ahead," *IEEE J. Sel. Areas Commun.*, vol. 38, no. 11, pp. 2450–2525, Nov. 2020.

[2] B. Zheng, C. You, W. Mei, and R. Zhang, "A survey on channel estimation and practical passive beamforming design for intelligent reflecting surface aided wireless communications," 2021, *arXiv:2110.01292*.

[3] Q. Wu and R. Zhang, "Towards smart and reconfigurable environment: Intelligent reflecting surface aided wireless network," *IEEE Commun. Mag.*, vol. 58, no. 1, pp. 106–112, Jan. 2020.

[4] Q. Wu, S. Zhang, B. Zheng, C. You, and R. Zhang, "Intelligent reflecting surface-aided wireless communications: A tutorial," *IEEE Trans. Commun.*, vol. 69, no. 5, pp. 3313–3351, May 2021.

[5] Q. Wu and R. Zhang, "Intelligent reflecting surface enhanced wireless network via joint active and passive beamforming," *IEEE Trans. Wireless Commun.*, vol. 18, no. 11, pp. 5394–5409, Nov. 2019.

[6] S. Zhang and R. Zhang, "Capacity characterization for intelligent reflecting surface aided MIMO communication," *IEEE J. Sel. Areas Commun.*, vol. 38, no. 8, pp. 1823–1838, Aug. 2020.

[7] C. Pan, H. Ren, K. Wang, W. Xu, M. Elkashlan, A. Nallanathan, and L. Hanzo, "Multicell MIMO communications relying on intelligent reflecting surfaces," *IEEE Trans. Wireless Commun.*, vol. 19, no. 8, pp. 5218–5233, Aug. 2020.

[8] Y. Yang, B. Zheng, S. Zhang, and R. Zhang, "Intelligent reflecting surface meets OFDM: Protocol design and rate maximization," *IEEE Trans. Commun.*, vol. 68, no. 7, pp. 4522–4535, Jul. 2020.

[9] B. Zheng, C. You, and R. Zhang, "Intelligent reflecting surface assisted multi-user OFDMA: Channel estimation and training design," *IEEE Trans. Wireless Commun.*, vol. 19, no. 12, pp. 8315–8329, Dec. 2020.

[10] B. Zheng and R. Zhang, "Intelligent reflecting surface-enhanced OFDM: Channel estimation and reflection optimization," *IEEE Wireless Commun. Lett.*, vol. 9, no. 4, pp. 518–522, Apr. 2020.

[11] F. Fang, Y. Xu, Q.-V. Pham, and Z. Ding, "Energy-efficient design of IRS-NOMA networks," *IEEE Trans. Veh. Technol.*, vol. 69, no. 11, pp. 14088–14092, Nov. 2020.

[12] B. Zheng, Q. Wu, and R. Zhang, "Intelligent reflecting surface-assisted multiple access with user pairing: NOMA or OMA?" *IEEE Commun. Lett.*, vol. 24, no. 4, pp. 753–757, Apr. 2020.

[13] Q. Wu and R. Zhang, "Weighted sum power maximization for intelligent reflecting surface aided SWIPT," *IEEE Wireless Commun. Lett.*, vol. 9, no. 5, pp. 586–590, May 2020.

[14] C. You, B. Zheng, and R. Zhang, "Channel estimation and passive beamforming for intelligent reflecting surface: Discrete phase shift and progressive refinement," *IEEE J. Sel. Areas Commun.*, vol. 38, no. 11, pp. 2604–2620, Nov. 2020.

[15] X. Guan, Q. Wu, and R. Zhang, "Anchor-assisted channel estimation for intelligent reflecting surface aided multiuser communication," *IEEE Trans. Wireless Commun.*, vol. 21, no. 6, pp. 3764–3778, Jun. 2022.

[16] B. Zheng, C. You, and R. Zhang, "Efficient channel estimation for double-IRS aided multi-user MIMO system," *IEEE Trans. Commun.*, vol. 69, no. 6, pp. 3818–3832, Jun. 2021.

[17] Z. Wang, L. Liu, and S. Cui, "Channel estimation for intelligent reflecting surface assisted multiuser communications: Framework, algorithms, and analysis," *IEEE Trans. Wireless Commun.*, vol. 19, no. 10, pp. 6607–6620, Oct. 2020.

[18] Z. Chen, J. Tang, X. Y. Zhang, D. K. C. So, S. Jin, and K.-K. Wong, "Hybrid evolutionary-based sparse channel estimation for IRS-assisted mmWave MIMO systems," *IEEE Trans. Wireless Commun.*, vol. 21, no. 3, pp. 1586–1601, Mar. 2022.

[19] Z.-Q. He and X. Yuan, "Cascaded channel estimation for large intelligent metasurface assisted massive MIMO," *IEEE Wireless Commun. Lett.*, vol. 9, no. 2, pp. 210–214, Feb. 2020.

[20] X. Hu, C. Zhong, Y. Zhang, X. Chen, and Z. Zhang, "Location information aided multiple intelligent reflecting surface systems," *IEEE Trans. Commun.*, vol. 68, no. 12, pp. 7948–7962, Dec. 2020.

[21] K. Zhi, C. Pan, H. Ren, and K. Wang, "Statistical CSI-based design for reconfigurable intelligent surface-aided massive MIMO systems with direct links," *IEEE Wireless Commun. Lett.*, vol. 10, no. 5, pp. 1128–1132, May 2021.

[22] G. Zhou, C. Pan, H. Ren, P. Popovski, and A. L. Swindlehurst, "Channel estimation for RIS-aided multiuser millimeter-wave systems," *IEEE Trans. Signal Process.*, vol. 70, pp. 1478–1492, 2022.

[23] P. Wang, J. Fang, W. Zhang, and H. Li, "Fast beam training and alignment for IRS-assisted millimeter wave/terahertz systems," *IEEE Trans. Wireless Commun.*, vol. 21, no. 4, pp. 2710–2724, Apr. 2022.

[24] Y. Lin, S. Jin, M. Matthaiou, and X. You, "Tensor-based algebraic channel estimation for hybrid IRS-assisted MIMO-OFDM," *IEEE Trans. Wireless Commun.*, vol. 20, no. 6, pp. 3770–3784, Jun. 2021.

[25] E. Basar, "Reconfigurable intelligent surfaces for Doppler effect and multipath fading mitigation," *Front. Comms. Net.*, vol. 2, May 2021, Art. no. 672857, doi: 10.3389/frcmn.2021.672857.

[26] S. Sun and H. Yan, "Channel estimation for reconfigurable intelligent surface-assisted wireless communications considering Doppler effect," *IEEE Wireless Commun. Lett.*, vol. 10, no. 4, pp. 790–794, Apr. 2021.

[27] Z. Huang, B. Zheng, and R. Zhang, "Roadside IRS-aided vehicular communication: Efficient channel estimation and low-complexity beamforming design," *IEEE Trans. Wireless Commun.*, vol. 22, no. 9, pp. 5976–5989, Sep. 2023.

[28] Y. Chen, Y. Wang, J. Zhang, P. Zhang, and L. Hanzo, "Reconfigurable intelligent surface (RIS)-aided vehicular networks: Their protocols, resource allocation, and performance," *IEEE Veh. Technol. Mag.*, vol. 17, no. 2, pp. 26–36, Jun. 2022.

[29] C. Hu, L. Dai, S. Han, and X. Wang, "Two-timescale channel estimation for reconfigurable intelligent surface aided wireless communications," *IEEE Trans. Commun.*, vol. 69, no. 11, pp. 7736–7747, Nov. 2021.

[30] Y. Chen, Y. Wang, Z. Wang, and P. Zhang, "Robust beamforming for active reconfigurable intelligent omni-surface in vehicular communications," *IEEE J. Sel. Areas Commun.*, vol. 40, no. 10, pp. 3086–3103, Oct. 2022.

[31] R. Zhang, L. Cheng, S. Wang, Y. Lou, Y. Gao, W. Wu, and D. W. K. Ng, "Integrated sensing and communication with massive MIMO: A unified tensor approach for channel and target parameter estimation," *IEEE Trans. Wireless Commun.*, vol. 23, no. 8, pp. 8571–8587, Aug. 2024, doi: 10.1109/TWC.2024.3351856.

[32] R. Zhang, L. Cheng, S. Wang, Y. Lou, W. Wu, and D. W. K. Ng, "Tensor decomposition-based channel estimation for hybrid mmWave massive MIMO in high-mobility scenarios," *IEEE Trans. Commun.*, vol. 70, no. 9, pp. 6325–6340, Sep. 2022.

[33] R. Zhang, L. Cheng, W. Zhang, X. Guan, Y. Cai, W. Wu, and R. Zhang, "Channel estimation for movable-antenna MIMO systems via tensor decomposition," 2024, *arXiv:2407.18773*.

[34] D. Needell and J. A. Tropp, "CoSaMP: Iterative signal recovery from incomplete and inaccurate samples," *Appl. Comput. Harmon. Anal.*, vol. 26, no. 3, pp. 301–321, May 2009.

[35] S. J. Julier and J. K. Uhlmann, "A new extension of the Kalman filter to nonlinear systems," *Proc. SPIE*, vol. 3068, pp. 182–193, Jul. 1997, doi: 10.1117/12.280797.

[36] J. B. Jorgensen P. G. Thomsen, H. Madsen, and M. R. Kristensen, "Computationally efficient and robust implementation of the continuous-discrete extended Kalman filter," in *Proc. Amer. Control Conf.*, New York, NY, USA, Jul. 2007, pp. 3706–3712.

[37] T. T. Cai and L. Wang, "Orthogonal matching pursuit for sparse signal recovery with noise," *IEEE Trans. Inf. Theory*, vol. 57, no. 7, pp. 4680–4688, Jul. 2011.

[38] S. F. Cotter and B. D. Rao, "Sparse channel estimation via matching pursuit with application to equalization," *IEEE Trans. Commun.*, vol. 50, no. 3, pp. 374–377, Mar. 2002.

[39] D. L. Donoho, Y. Tsaig, I. Drori, and J.-L. Starck, "Sparse solution of underdetermined systems of linear equations by stagewise orthogonal matching pursuit," *IEEE Trans. Inf. Theory*, vol. 58, no. 2, pp. 1094–1121, Feb. 2012.

[40] D. Needell and R. Vershynin, "Uniform uncertainty principle and signal recovery via regularized orthogonal matching pursuit," *Found. Comput. Math.*, vol. 9, pp. 317–334, Jun. 2009.

[41] P. Indyk and M. Ruzic, "Near-optimal sparse recovery in the L_1 norm," in *Proc. 49th Annu. IEEE Symp. Found. Comput. Sci.*, Oct. 2008, pp. 199–207.

[42] R. Berinde, P. Indyk, and M. Ruzic, "Practical near-optimal sparse recovery in the L_1 norm," in *Proc. 46th Annu. Allerton Conf. Commun., Control, Comput.*, Sep. 2008, pp. 198–205.

[43] H. V. Pham, W. Dai, and O. Milenkovic, "Sublinear compressive sensing reconstruction via belief propagation decoding," in *Proc. IEEE Int. Symp. Inf. Theory*, Jun. 2009, pp. 674–678.

[44] S. S. Chen, D. L. Donoho, and M. A. Saunders, "Atomic decomposition by basis pursuit," *SIAM Rev.*, vol. 43, no. 1, pp. 129–159, Jan. 2001.

[45] G. Destino, M. Juntti, and S. Nagaraj, "Leveraging sparsity into massive MIMO channel estimation with the adaptive-LASSO," in *Proc. IEEE Global Conf. Signal Inf. Process. (GlobalSIP)*, Dec. 2015, pp. 166–170.

[46] X. Wei, D. Shen, and L. Dai, "Channel estimation for RIS assisted wireless communications—Part II: An improved solution based on double-structured sparsity," *IEEE Commun. Lett.*, vol. 25, no. 5, pp. 1403–1407, May 2021.

[47] G. Welch and G. Bishop, "An introduction to the Kalman filter," Dept. Comput. Sci., Univ. North Carolina at Chapel Hill, Chapel Hill, NC, USA, Tech. Rep. 27599-3175, 3175.

[48] H. Zhang, G. Dai, J. Sun, and Y. Zhao, "Unscented Kalman filter and its nonlinear application for tracking a moving target," *Optik*, vol. 124, no. 20, pp. 4468–4471, Oct. 2013.

[49] Y. Boers and J. N. Driessen, "Particle filter based detection for tracking," in *Proc. Amer. Control Conf.*, Arlington, VA, USA, 2001, pp. 4393–4397, doi: 10.1109/acc.2001.945669.

S. NANDAN (Senior Member, IEEE) received the bachelor's degree from Kerala University and the master's degree from the National Institute of Technology, Calicut, Kerala. He is currently an Assistant Professor with the Department of Electronics and Communication Engineering, LBS Institute of Technology for Women, Trivandrum, Kerala, a Government of Kerala Undertaking Institution, under APJ Abdul Kalam Technological University, Kerala, India. His research interests include wireless communication, 5G mobile communications, intelligent reflective surfaces, and MIMO OFDM systems for communication.

M. ABDUL RAHIMAN received the Bachelor of Technology degree from Calicut University, the Master of Technology degree from Kerala University, and the Ph.D. degree from Karpagam Deemed to be University. He was a first Pro Vice Chancellor of APJ Abdul Kalam Technological University, Kerala, India. He is currently the Director of the LBS Centre for Science & Technology, a Government of Kerala Undertaking Organization. He is also a Principal and a Professor with the Department of Computer Science Engineering, LBS Institute of Technology for Women, Trivandrum, Kerala, under APJ Abdul Kalam Technological University, Kerala. He was the former Director, All India Council for Technical Education (AICTE), the Apex Body of Technical Education under Ministry of Human Resource Development, Government of India, and the Director of VHSE, Government of Kerala. His research interests include digital image processing, wireless communication, 5G mobile communications, machine learning, and data mining.